Capillary Forces between Colloidal Particles

Peter A. Kralchevsky† and Kuniaki Nagayama*

Protein Array Project, ERATO, JRDC, 18-1 Higashiarai, Tsukuba 305, Japan

Received December 10, 1992. In Final Form: September 14, 1993®

This work is devoted to a special kind of capillary interaction, which differs from the common lateral capillary forces between floating particles. It appears between particles protruding from a liquid film and its physical origin is the capillary rise of the liquid along the surface of each particle. Special attention is paid to the case when the position of the contact line is fixed. The resulting capillary force is compared with that at fixed contact angle. It is demonstrated that the two alternative approaches to the calculation of capillary interactions, the force and the energetical one, are equivalent. When the liquid film is thin, the disjoining pressure affects the capillary interactions between particles attached to the film surfaces. The appearance of this effect is studied quantitatively for two specified systems modeling globular proteins in aqueous film on mercury substrate and membrane proteins incorporated in a lipid bilayer. For both systems the capillary forces appear to be strong enough to engender two-dimensional particle aggregation and ordering. This is a possible explanation of a number of experimental observations of such effects.

Introduction

A new interest in the capillary interaction between colloidal particles has been aroused by the experimental findings that it can produce formation of two-dimensional arrays from submicrometer particles.[1,2] This interaction differs from the conventional lateral capillary force between floating particles in two aspects: (i) it is operative with very *small particles* (even down to 10 nm size) and (ii) it appears between particles, which are partially immersed in a *liquid film*.[3] In particular, it was observed[1,2] that the transition from disordered state (Figure 1a) forward to ordered state (Figure 1b) appears suddenly in the moment, when the particle tops protrude from the thinning liquid films. The role of gravity in this case is to keep the film surface planar. This role is played by the disjoining pressure when the film is thin enough.[3] In the latter case the capillary interactions between colloidal particles are entirely governed by the surface forces (those which give rise to the disjoining pressure and the three-phase contact angle), the gravity effect being negligible.

Recent experiments[4-6] show that globular protein macromolecules form a two-dimensional ordered array in an aqueous film spread on a substrate. The occurrence of this phenomenon with proteins[4,5] in many aspects resembles the ordering process with the larger latex particles[1,2] (Figure 1). It can be expected that the capillary interparticle forces play an important role in both these systems. It should be noted that well-ordered two-dimensional protein arrays are the subject of intensive research as a basis of future high technologies at a macromolecular level.[7]

The capillary forces between particles attached to an interface were studied experimentally by Hinsch[8] and Camoin *et al.*[9] and theoretically by Nicolson,[10] Gifford and Scriven,[11] Chan *et al.*,[12] and Fortes.[13] The theoretical approach developed in ref 3 for identical particles was later extended to particles of different size and contact angle[14] and to particle–wall interactions.[15]

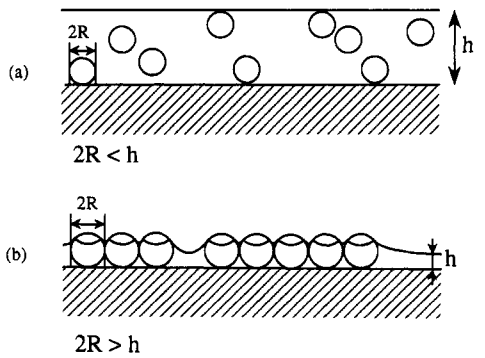

Figure 1. Two-dimensional ordering of suspension particles in a liquid layer on a substrate: (a) chaotic motion of the particles in a thick layer; (b) the capillary forces appear and give rise to aggregation after the particle tops protrude form the liquid layer.

In the present paper we first investigate the similarities and dissimilarities between the different kinds of capillary forces. Our aim is to attract the reader's attention to the variety of capillary interactions and their physical importance. In particular, we compare the magnitudes of the capillary interactions taking place at two different boundary conditions on the particle surfaces: fixed contact angle and fixed contact line. However, our main purpose in this article is to investigate some general properties of the lateral capillary forces. In fact, we deal with an *indirect* interaction stemming from the overlap of the perturbations in the meniscus shape, which are due to the presence of attached particles. Therefore, a theoretical description of the capillary interaction resembling a two-dimensional

* Author to whom correspondence should be addressed.
† Permanent address: Faculty of Chemistry, University of Sofia, 1126 Sofia, Bulgaria.
® Abstract published in *Advance ACS Abstracts*, November 1, 1993.

(1) Denkov, N. D.; Velev, O. D.; Kralchevsky, P. A.; Ivanov, I. B.; Yoshimura, H.; Nagayama, K. *Nature (London)* **1993**, *361*, 26.
(2) Denkov, N. D.; Velev, O. D.; Kralchevsky, P. A.; Ivanov, I. B.; Yoshimura, H.; Nagayama, K. *Langmuir* **1992**, *8*, 3183.
(3) Kralchevsky, P. A.; Paunov, V. N.; Inanov, I. B.; Nagayama, K. *J. Colloid Interface Sci.* **1992**, *151*, 79.
(4) Yoshimura, H.; Endo, S.; Matsumoto, M.; Nagayama, K.; Kagawa, Y. *J. Biochem.* **1989**, *106*, 958.
(5) Yoshimura, H.; Matsumoto, M.; Endo, S.; Nagayama, K. *Ultramicroscopy* **1990**, *32*, 265.
(6) Haggerty, L.; Yoshimura, H.; Watson, B. A.; Barteau, M. A.; Lenhoff, A. M. *J. Vac. Sci. Technol.* **1991**, *B9*, 1219.
(7) Nagayama, K. *Nanobiology* **1992**, *1*, 25.
(8) Hinsch, K. *J. Colloid Interface Sci.* **1983**, *92*, 243.
(9) Camoin, C.; Roussel, J. F.; Faure, R.; Blanc, R. *Europhys. Lett.* **1987**, *3*, 449.
(10) Nicolson, M. M. *Proc. Cambridge Philos. Soc.* **1949**, *45*, 288.
(11) Gifford, W. A.; Scriven, L. E. *Chem. Eng. Sci.* **1971**, *26*, 287.
(12) Chan, D. Y. C.; Henry, J. D.; White, L. R. *J. Colloid Interface Sci.* **1981**, *79*, 410.
(13) Fortes, M. A. *Can. J. Chem.* **1982**, *60*, 2889.
(14) Kralchevsky, P. A.; Paunov, V. N.; Denkov, N. D.; Ivanov, I. B.; Nagayama, K. *J. Colloid Interface Sci.* **1993**, *155*, 420.
(15) Paunov, V. N.; Kralchevsky, P. A.; Denkov, N. D.; Ivanov, I. B.; Nagayama, K. *Colloids Surf.* **1992**, *67*, 119.

0743-7463/94/2410-0023$04.50/0

field theory is possible. In this aspect, a general proof is given to an analogue of Newton's third law for capillary forces between particles attached to the surface of both thick and thin liquids films. In the latter case the effect of the *disjoining pressure* is taken into account. Then we demonstrate analytically the equivalence between the two alternative theoretical approaches to the capillary interactions: the energetical and the force one, which have been previously found[14,16] to give numerically coinciding results. Finally, we study quantitatively the capillary interactions in two specified systems modeling the experiments with globular proteins in aqueous films on mercury[4,5] and with membrane proteins incorporated in phospholipid bilayers (biomembranes) in an aqueous environment.[17-20] Our aim is to verify whether the lateral capillary forces in these systems are strong enough to produce two-dimensional particle aggregation.

Capillary Forces: Theoretical Description

Many works have been devoted to the theoretical description of the capillary forces,[10-16] but because of the diversity of the approaches and configurations studied an outline is needed.

Flotation and Immersion Lateral Capillary Forces. The cause of the lateral capillary forces is the *deformation* of the liquid surface, which is supposed to be flat in the absence of particles. The larger the interfacial deformation created by the particles, the stronger the capillary interaction between them. It is known that two similar particles floating on a liquid interface attract each other; see Figure 2a and refs 12, 13, and 16. This attraction appears because the liquid meniscus deforms in such a way that the gravitational potential energy of the two particles decreases when they approach each other. Hence the origin of this force is the *particle weight* (plus the Archimedes force).

A force of capillary attraction appears also when the particles (instead of being freely floating) are partially immersed in a liquid layer on a substrate; see Figure 2b and refs 3 and 14. The deformation of the liquid surface in this case is related to the *wetting properties* of the particle surface, i.e. to the position of the contact line and the magnitude of the contact angle, rather than to gravity.

To distinguish the capillary forces in the case of floating particles from ones in the case of partially immersed particles on a substrate, we call the former lateral *flotation* forces and the latter lateral *immersion* forces. As demonstrated below (eq 1.29) the flotation and immersion forces exhibit similar dependence on the interparticle separation and different dependencies on the particle radius and the surface tension of the liquid.

The flotation and immersion forces can be both attractive (Figure 2a,b) and repulsive (Figure 2c,d). This is determined by the signs of the meniscus slope angles Ψ_1 and Ψ_2 at the two contact lines: the capillary force is attractive when $\sin\Psi_1 \sin\Psi_2 > 0$ and repulsive when $\sin\Psi_1 \sin\Psi_2 < 0$; see refs 14 and 16 for detail. The sign of Ψ_1 or Ψ_2, separately, is a matter of convention; we follow the convention $\Psi > 0$ ($\Psi < 0$) for convex (concave) meniscus. In the case of flotation forces $\Psi > 0$ for *light* particles (including bubbles) and $\Psi < 0$ for *heavy* particles. In the case of immersion forces between particles protruding from an aqueous layer $\Psi > 0$ for *hydrophilic* particles and $\Psi < 0$ for *hydrophobic* particles. When $\Psi = 0$ there is no meniscus deformation and hence there is no capillary interaction between the particles. This can happen when the weight of the particles is too small to create significant surface deformation—see Figure 2e: the depth of the particles immersion is determined by the magnitude of the contact angles α_1 and α_2. Such is the situation with particles of radii smaller than ca. 10 μm, when the interaction energy due to *flotation* force becomes smaller than the thermal energy kT (cf. Figure 7 below). On the other hand, the *immersion* force can be significant even with 10 nm large colloidal particles confined in a thin liquid film, Figure 2f. In this case the film surfaces (far enough from the particles) are kept plane-parallel by the disjoining pressure rather than by gravity.[3] The immersion force is responsible for the assembling of micrometer size particles in thin liquid films[1,2] as sketched in Figure 1.

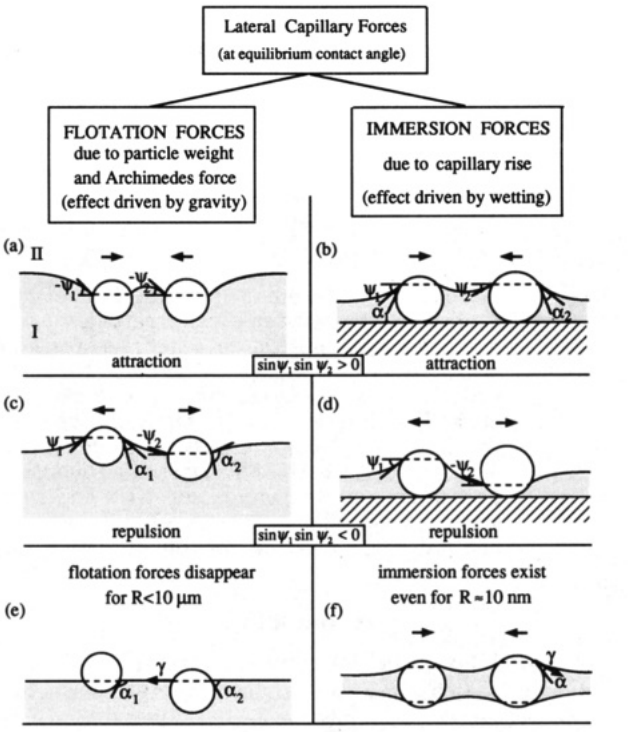

Figure 2. Comparison between the flotation (a, c, e) and immersion (b, d, f) lateral capillary forces. Ψ_1 and Ψ_2 are meniscus slope angles; α_1 and α_2 are contact angles; γ is interfacial tension. The flotation force appears between freely floating particles whereas the immersion force appears when particles are partially immersed in a liquid film.

It is worthwhile noting that the immersion force between particles confined in a thin liquid film is substantial even when the contact angle α is zero[3] (pronouncedly wettable particle surface). On the other hand, flotation forces cannot be observed with $\alpha = 0$ because the particles will detach from the interface and will sink into the lower liquid.

Immersion type lateral capillary force can appear not only between two particles but also between two partially immersed vertical cylinders, which cannot move along the vertical;[3,14,15] see Figure 3. A construction of this type is convenient for a direct measurement of the immersion force and has been used in the experiments of Camoin *et al.*[9]

Force and Energetical Approaches to Capillary Interactions. There are two alternative theoretical methods for calculating the lateral capillary interactions: the energetical[3,12,16] and the force[14,15] approaches.

The *energetical* approach is based on a general expression for the grand thermodynamic potential of a system

(16) Paunov, V. N.; Kralchevsky, P. A.; Denkov, N. D.; Nagayama, K. *J. Colloid Interface Sci.* **1993**, *157*, 100.
(17) Chen, Y. S.; Hubbell, W. L. *Exp. Eye Res.* **1973**, *17*, 517.
(18) Lewis, B. A.; Engelman, D. M. *J. Mol. Biol.* **1983**, *166*, 203.
(19) Aebi, U.; Fowler, W. E.; Loren-Buhle, E. J.; Smith, P. R. *J. Ultrastruct. Res.* **1984**, *88*, 143.
(20) Baldwin, J. M.; Henderson, R.; Beckman, E. I.; Zemlin, F. *J. Mol. Biol.* **1988**, *202*, 585.

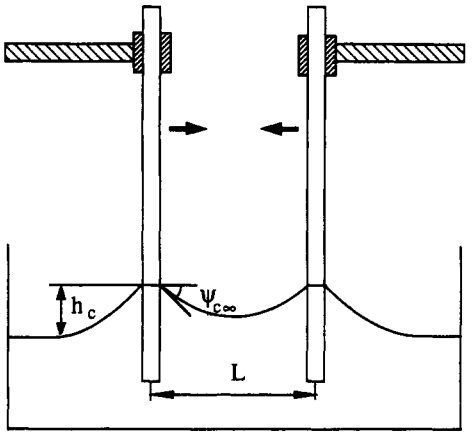

Figure 3. Sketch of two vertical cylinders separated at a distance L, which are partially immersed in a liquid; $\Psi_{c\infty}$ is the meniscus slope angle at the contact line and h_c is its elevation above the planar liquid surface far from the cylinders. The overlap of the menisci on the two cylinders gives rise to a lateral capillary force liable to a direct measurement.

of particles attached to the interface between fluid I and fluid II (see, e.g., Figure 2a)[3]

$$\Omega(\mathbf{r}_1,...,\mathbf{r}_N) = \sum_{K=1}^{N} m_K g Z_K^{(c)} - \sum_{Y=I,II} \int_{V_Y} P_Y \, dV + \sum_{K=1}^{N} \sum_{Y=I,II} \omega_{KY} A_{KY} + \gamma A + \text{const} \quad (1.1)$$

Here $\mathbf{r}_1, \mathbf{r}_2, ..., \mathbf{r}_N$ are the position vectors of the particle mass centers and m_K values ($K = 1, 2, ..., N$) are their masses; $Z_K^{(c)}$ is the projection of $\mathbf{r}_K$ along the vertical; g is the acceleration due to gravity; P_Y and V_Y are the pressure and volume of fluid phase Y ($Y = I, II$); A_{KY} and ω_{KY} are the area and the surface free energy density of the interface between particle K and phase Y; γ and A are the interfacial tension and the area of the boundary between fluids I and II; the additive constant in eq 1.1 does not depend on $\mathbf{r}_1, \mathbf{r}_2, ..., \mathbf{r}_N$. Then the lateral capillary force between particles 1 and 2 is determined by differentiation:

$$F^{(12)} = -\frac{\partial \Omega}{\partial r_{12}}, \qquad r_{12} = |\mathbf{r}_1 - \mathbf{r}_2| \quad (1.2)$$

The pressure in eq 1.1 depends on the vertical coordinate, z, due to the gravity effect

$$P_Y = P_{Y0} - \rho_Y g z, \qquad P_{Y0} \equiv P_Y|_{z=0} = \text{const}, \qquad Y = I, II \quad (1.3)$$

where ρ_I and ρ_{II} are the mass densities of the respective fluids.

In the alternative *force* approach the lateral capillary force exerted on one of the particles is calculated by integrating the meniscus interfacial tension along the contact line and the hydrostatic pressure throughout the particle surface:

$$\mathbf{F}^{(k)} = \mathbf{F}^{(k\gamma)} + \mathbf{F}^{(kp)}, \qquad k = 1, 2, ... \quad (1.4)$$

where

$$\mathbf{F}^{(k\gamma)} = \mathbf{U}_{II} \cdot \oint_{L_k} dl \, \mathbf{u} \gamma \quad (1.5)$$

is the contribution of the interfacial tension and

$$\mathbf{F}^{(kp)} = \mathbf{U}_{II} \cdot \oint_{S_k} ds(-\mathbf{n}P) \quad (1.6)$$

is the contribution of the hydrostatic pressure. Here L_k is the three-phase contact line, S_k denotes the particle surface with outer unit running normal $\mathbf{n}$, dl and ds are linear and surface elements and $\mathbf{U}_{II}$ is the unit tensor (idemfactor) of the horizontal plane xy, and $\mathbf{u}$ is the running unit normal to the contact line, which is tangential to the meniscus surface; $\mathbf{u}$ determines the direction of the surface tension force exerted on the particle along the contact line. The meaning of eqs 1.4–1.6 is illustrated in Figure 4 for the case of two particles on substrate. One can realize that if the contact lines were horizontal, both $\mathbf{F}^{(kp)}$ and $\mathbf{F}^{(k\gamma)}$ ($k = 1, 2$) would be zero. In fact the lateral capillary force $\mathbf{F}^{(k)}$ is a result of the perturbation of the shape of the liquid meniscus around a given particle caused by the presence of the second particle. The calculations carried out in refs 14 and 16 show that $|\mathbf{F}^{(kp)}| \ll |\mathbf{F}^{(k\gamma)}|$ with submillimeter particles; that is, the interfacial tension contribution dominates the lateral capillary force. As far as the two particles interacting indirectly through the perturbation in the shape of the liquid meniscus created by them, it is not quite obvious that a counterpart of Newton's third law will hold, i.e. that

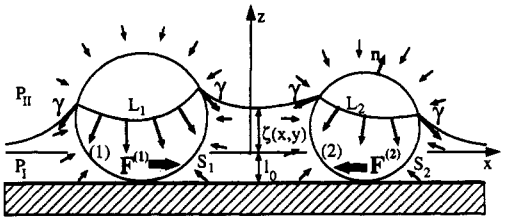

Figure 4. The lateral capillary force $\mathbf{F}^{(k)}$ is a net force originating from the integral of surface tension γ along the contact line L_k and the integral of hydrostatic pressure throughout the particle surface S_k ($k = 1, 2$); l_0 is the thickness of the plane-parallel liquid layer far from the particles; P_I and P_{II} are the pressures in phases I and II; $z = \zeta(x,y)$ determines the meniscus shape.

$$\mathbf{F}^{(1)} = -\mathbf{F}^{(2)} \quad (1.7)$$

A general derivation of eq 1.7 is given below in this paper; see eqs 2.17 and 3.9.

Besides, it is not obvious that the energetical and force approaches are equivalent, i.e. that the magnitudes of the capillary force calculated by means of eqs 1.2 and 1.4 will coincide. Numerical coincidence of the results of these two approaches was established in refs 14 and 16. Below one can find analytical proof of the equivalence of the energetical and force approaches.

Boundary Conditions at the Contact Line. Let us consider a system of two particles attached to the interface between phases I and II; this can be each of the configurations depicted in Figures 2–4. The fluid interface is supposed to be flat and horizontal far from the particles. We choose the coordinate plane xy to coincide with this horizontal surface. Let

$$z = \zeta(x,y) \quad (1.8)$$

be the equation describing the shape of the liquid meniscus formed around the two particles. In general, the meniscus shape obeys the Laplace equation of capillarity[21]

$$2H\gamma = (P_{II} - P_I)_{z=\zeta} \quad (1.9)$$

where H is the meniscus mean curvature. Since the meniscus is flat far from the particles, $P_{I0} = P_{II0}$ in eq 1.3 and then eq 1.9 can be transformed to read

$$2H \equiv \nabla_{II} \cdot \left[\frac{\nabla_{II}\zeta}{(1 + |\nabla_{II}\zeta|^2)^{1/2}} \right] = q^2 \zeta \quad (1.10)$$

where the representation of the mean curvature as a two-

(21) Princen, H. M. In *Surface and Colloid Science*; Matijevic, E., Ed.; Wiley: New York, 1969; Vol. 2, p 1.

dimensional divergence[22] has been used. Here

$$\nabla_{II} = \left(\frac{\partial}{\partial x}, \frac{\partial}{\partial y}\right) \tag{1.11}$$

is the gradient operator in the plane xy and

$$q^{-1} = \left(\frac{\gamma}{\Delta\rho g}\right)^{1/2} \qquad (\Delta\rho = \rho_I - \rho_{II}) \tag{1.12}$$

is the capillary length. For a water–air interface at room temperature $q^{-1} = 2.7$ mm. In fact q^{-1} determines the range of the lateral capillary forces (see eq 1.26 below). Equation 1.10 represents a second-order differential equation for determining ζ. In our case, one of the boundary conditions reads

$$\lim_{r\to\infty} \zeta(x,y) = 0, \qquad r = (x^2 + y^2)^{1/2} \tag{1.13}$$

The other boundary condition, which is imposed at the three-phase contact lines on the particle surfaces, depends on the specified physical conditions. Most frequently formation of a constant contact angle, α, is supposed. Such an angle satisfies the Young equation

$$\omega_{k,II} - \omega_{k,I} = \gamma \cos \alpha_k, \qquad k = 1, 2 \tag{1.14}$$

In the case of vertical cylinders, like those depicted in Figure 3, the boundary condition reads

$$\mathbf{m}\cdot\nabla_{II}\zeta = -\cot \alpha_k = \text{const} \qquad \text{(at contact line } L_k,\ k = 1, 2) \tag{1.15}$$

where $\mathbf{m}$ is the outer unit normal of the cylindrical surface. Equation 1.15 determines the meniscus *slope* at the contact line.

Other possible physical situation is the meniscus *position*, rather than the meniscus *slope*, to be fixed at the contact line. As sketched in Figure 5a,b this can happen when the contact line is located at some edge on the particle surface. Another possibility is the contact line to be attached to the boundary between hydrophilic and lipophilic domains of the surface, as shown in Figure 5c. Similar configuration can be observed with membrane proteins incorporated in a lipid film in water, when the hydrophilic ends of the protein molecules (the shadowed caps in Figure 5c) protrude from the lipid film. Such proteins are found to attract each other and to form two-dimensional ordered array.[17–20] Note that in the three configurations depicted in Figure 2a–c the interaction belongs to the *immersion* type of lateral capillary force. The boundary condition at the contact line in the case of consideration reads

$$\zeta = h_{c\infty} = \text{const} \qquad \text{(at the contact line)} \tag{1.16}$$

cf. Figure 5.

When the liquid film is thin enough the *disjoining pressure* effect becomes important. Then if the meniscus slope is small, the meniscus profile $\zeta(x,y)$ can be found by solving eq 1.10, where q is defined as follows:[3]

$$q^2 = \frac{\Delta\rho g}{\gamma} - \frac{\Pi'}{\gamma}, \qquad \Pi' \equiv \left.\frac{d\Pi}{dh}\right|_{\zeta=0} \tag{1.17}$$

Here $\Pi(h)$ is the disjoining pressure isotherm with h being the film thickness. $\Pi \to 0$ for large h and then eq 1.17 reduces to eq 1.12. On the contrary, one has $-\Pi' \gg \Delta\rho g$ in *thin* films and then the gravitational term in eq 1.17 becomes negligible. As shown in ref 3, to derive eq 1.17 one first expands Π in series for $\zeta \ll h$ and then neglects the quadratic and higher order terms with respect to ζ.

(22) Finn, R. *Equilibrium Capillary Surfaces*; Springer-Verlag: New York, 1986.

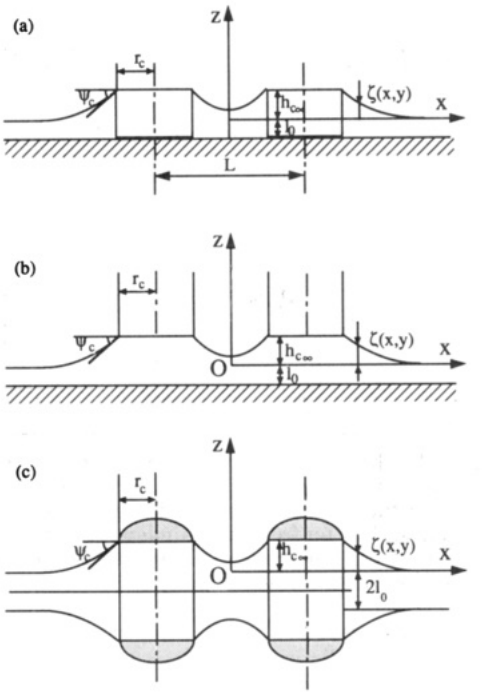

Figure 5. Capillary interactions at fixed position of the contact line: (a) two vertical cylinders or disks immersed in a liquid layer; (b) two vertical cylinders whose lower bases are attached to a fluid interface; (c) particles incorporated in an emulsion film: the contact lines are attached to the boundaries between the hydrophilic and lipophilic domains of the particle surface. As the contact lines are immobilized, the energy of wetting does not contribute to the capillary interaction, unlike the cases with mobile contact lines depicted in Figures 2 and 3.

To compare the magnitudes of the lateral capillary forces corresponding to the two alternative boundary conditions, eq 1.15 (fixed slope) and eq 1.16 (fixed elevation), let us consider the simplest geometry: two vertical cylinders of identical radii, r_c, at small meniscus slope:

$$|\nabla_{II}\zeta|^2 \ll 1 \tag{1.18}$$

In the case of fixed slope (eq 1.15) the interaction energy due to the lateral immersion force reads[3]

$$\Delta\Omega(L) = -2\pi\gamma r_c \sin \Psi_{c\infty}[h_c(L) - h_{c\infty}] \qquad \text{(fixed slope)} \tag{1.19}$$

where L is the distance between the axes of the two cylinders, $\sin \Psi_{c\infty} = \cos \alpha$, and $h_c(L)$ is the elevation of the contact line above the level of the plane liquid surface far from the cylinders; see Figure 3. Equation 1.19 is valid not only for thick but also for thin films, when disjoining pressure effects become important (see Appendix IV). In eq 1.19 we have used $\Delta\Omega$ instead of Ω to notify that the additive constant in eq 1.1 is determined in such a way that $\Delta\Omega \to 0$ when $L \to \infty$. $h_{c\infty}$ is the limiting value of h_c at $L \to \infty$, which is determined by Derjaguin's formula[23]

$$h_{c\infty} = r_c \sin \Psi_{c\infty} \ln \frac{2}{\gamma_e q r_c} \tag{1.20}$$

$$q r_c \ll 1$$

where $\gamma_e = 1.781072418...$ ($\ln \gamma_e = 0.577 ...$ is often called the Euler constant; see, e.g., ref 24, Chapter 6). On the other hand, as derived in ref 3

(23) Derjaguin, B. V. *Dokl. Acad. Nauk USSR* **1946**, *51*, 517.
(24) Abramowitz, M.; Stegun, I. A. *Handbook of Mathematical Functions*; Dover: New York, 1965.

$$h_c = r_c \sin \Psi_{c\infty}\left[\tau_c + 2 \ln \frac{1-\exp(-2\tau_c)}{\gamma_e q a}\right] \quad (1.21)$$

$$(qa)^2 \ll 1$$

where

$$a = (L^2/4 - r_c^2)^{1/2} \quad (1.22)$$

and

$$\tau_c = \ln[a/r_c + (1 + a^2/r_c^2)^{1/2}] \quad (1.23)$$

When the boundary condition of fixed elevation, eq 1.16, is used, the term $\sum \omega_{KY} A_{KY}$ in eq 1.1 is constant. Then by applying the procedure developed in ref 3 from eq 1.1, one derives the following expression for the capillary interaction energy between the two cylinders:

$$\Delta\Omega(L) = 2\pi\gamma r_c h_{c\infty}[\sin \Psi_c(L) - \sin \Psi_{c\infty}] \quad \text{(fixed elevation)} \quad (1.24)$$

see also Figure 5. (In the case of symmetric film, Figure 5c, there are two deformed liquid interfaces and consequently the interaction energy is twice $\Delta\Omega$ as given by eq 1.24.) To obtain analytical expression for $\Psi_c(L)$ we solved the Laplace equation, eq 1.10, under the restriction for small slope, eq 1.18. The derivation is presented in Appendix I, where one can also find analytical expression for the meniscus shape, $\zeta(x,y)$, of the configurations depicted in Figure 5. The result for sin $\Psi_c(L)$, which is to be substituted in eq 1.24, reads

$$\sin \Psi_c(L) = \left\{\frac{r_c}{A} + \left[K_0(qL) - \ln \frac{2}{\gamma_e q L}\right]\frac{r_c}{h_{c\infty}}\right\}^{-1} \quad (1.25)$$

$$(qr_c)^2 \ll 1$$

where K_0 is modified Bessel function and A is given by eq A.8 in Appendix I. (When the relationship A.19 is satisfied, eq A.18 should be used instead of eq 1.25 to calculate sin $\Psi_c(L)$.) Note that eq 1.24 is valid not only for thick but also for thin films, where disjoining pressure effects become important (see Appendix IV).

The energies of capillary interaction stemming from the two alternative boundary conditions, eqs 1.15 and 1.16, are compared in Figure 6. In both cases $\Delta\Omega$ is negative (attractive) and of the order of 10^{-12} J by magnitude (much greater than the thermal energy kT). The capillary interaction at constant slope turns out to be stronger than those at constant elevation.

Analytical Expressions for the Lateral Capillary Forces. Analytical expressions are available only for the case of small meniscus slope, when eq 1.18 holds and the Laplace equation, 1.10, can be linearized. Then a zeroth-order compound asymptotic expansion can be derived, which gives the following expression for the capillary force (for details see refs 14 and 16)

$$F = 2\pi\gamma Q_1 Q_2 q K_1(qL) \quad (1.26)$$

where K_1 is modified Bessel function

$$Q_k = r_k \sin \Psi_k, \qquad k = 1, 2 \quad (1.27)$$

r_k and Ψ_k, $k = 1, 2$, are the contact lines radii of the two interacting particles and meniscus slope angles. Note that eq 1.26 is derived under the *constant slope* boundary condition, eq 1.15. In the case of *constant elevation* it can be proven by means of eqs 1.2, 1.22, 1.24, and A.18 that eq 1.26 represents the asymptotic behavior of F at certain conditions (when $\epsilon \ll 1$ in eq A.19). It follows from eq 1.26 that

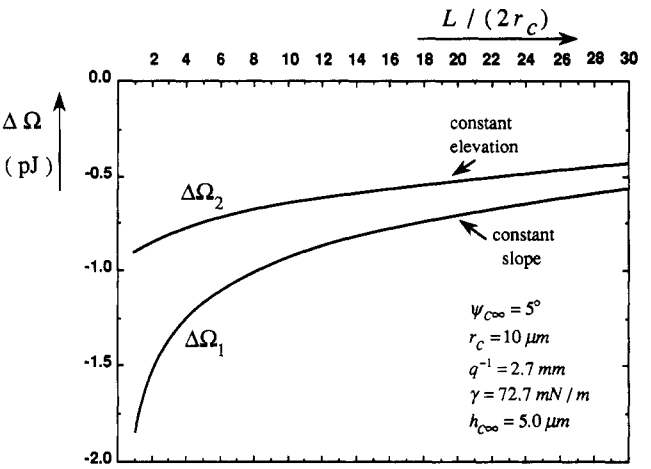

Figure 6. Free energy of capillary interaction $\Delta\Omega$ vs distance, L, between two vertical cylinders of radii r_c. $\Delta\Omega_1$ and $\Delta\Omega_2$ correspond to fixed slope (eq 1.19) and fixed elevation (eq 1.24), respectively. $\Psi_{c\infty}$ and $h_{c\infty}$ are the meniscus slope and the contact line elevation for a single cylinder ($L \to \infty$); γ is the meniscus surface tension and q^{-1} is the capillary length; cf. eq 1.12. The values of $\Psi_{c\infty}$, r_c, q^{-1}, γ, and $h_{c\infty}$ are the same for the two curves.

$$F = 2\pi\gamma \frac{Q_1 Q_2}{L}, \qquad \text{when } r_k \ll L \ll q^{-1} \quad (1.28)$$

Equation 1.28 resembles to some extent Coulomb's law of electricity. That is why Q_k is called[16] the "capillary charge" of particle k. In fact Q_k characterizes the ability of the particle to deform the liquid interface and thus to take part in capillary interactions.

In the simplest case of two vertical cylinders at constant contact angles (Figure 3) Q_k is a constant determined by the cylinder radius r_k and the contact angle $\alpha_k = \pi/2 - \Psi_k$; cf. eq 1.27.

The procedure of calculation of Q_k is the case of fixed contact angle is described in ref 3. In particular one has ($R_1 = R_2 = R$; $r_k \ll L \ll q^{-1}$)

$$F \propto \frac{R^6}{\gamma} K_1(qL) \text{ for flotation force}$$

$$F \propto \gamma R^2 K_1(qL) \text{ for immersion force} \quad (1.29)$$

Hence, the flotation force increases when the interfacial tension decreases. This is due to the fact that at given particle weight the meniscus deformation is larger when γ is lower; cf. Figure 2a,b. On the other hand, the immersion force increases proportionally to γ. This can be attributed to the fact that at a given capillary rise (and meniscus deformation) the meniscus surface energy is larger when γ is higher; cf. Figure 2b,d,f.

Equation 1.29 shows also that the flotation force decreases much stronger with the decrease of particle radius R than the immersion force. This is illustrated in Figure 7. The energy $\Delta\Omega$ due to *flotation* force is calculated for two identical floating spherical particles of mass density $\rho_1 = \rho_2 = \rho_P = 5$ g/cm^3 by integrating eq 1.26. The energy due to *immersion* force is calculated for two identical spherical particles on a substrate which are partially immersed in a liquid layer. Its thickness is uniform far from the particles and equal to $R/2$ ($l_0 = R/2$; cf. Figure 4); the calculation procedure is described in ref 3; the disjoining pressure effect is not taken into account. For both lines in Figure 7 the interparticle center-to-center distance is $L = 4R$. The energy of capillary interaction is

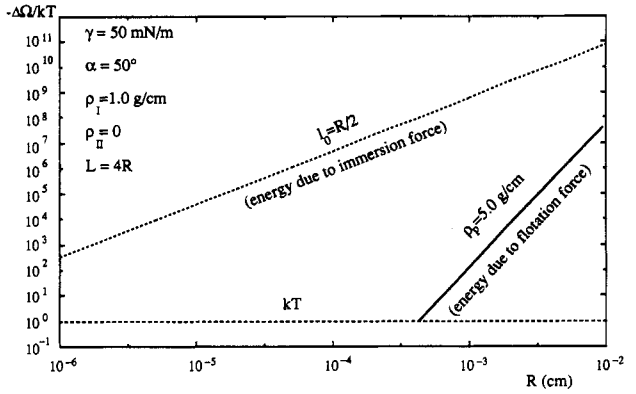

Figure 7. Free energy of capillary interaction, $\Delta\Omega$, between two identical spherical particles of radius R separated at a center-to-center distance $L = 4R$. The full and the dashed lines correspond to the particle configurations depicted in parts a (flotation force) and b (immersion force) of Figure 2, respectively. γ is the meniscus surface tension and α is the particle contact angle (Figure 2), l_0 is the thickness of the planar film far from the particles (Figure 4), ρ_p, ρ_I, and ρ_{II} are the mass densities of the particles and the two fluid phases I and II, respectively. The values of γ, α, ρ_I, ρ_{II}, and L are the same for the two lines.

divided by the thermal energy kT at room temperature (25 °C). One sees that the energy due to the flotation force decreases faster with the decrease of R and becomes smaller than kT (i.e. negligible) for $R < 7$ μm. On the other hand, the energy due to the *immersion* force is much larger than kT even for $R = 10$ nm. Hence it is possible for the immersion force to cause formation of two-dimensional aggregates (Figure 1b) of micrometer and submicrometer particles as observed experimentally.[1,2,5]

As mentioned above, analytical expressions for the lateral capillary forces are available in the case of *small meniscus slope*, when the Laplace equation can be linearized. For the readers convenience in Table I we list the configurations, for which analytical expressions are available, as well as the respective references in which details can be found.

Newton's Third Law for Capillary Forces: Thick Films

As known from hydraulics, when two pistons of different area contact with a liquid under pressure, the force exerted on the piston of larger area is larger. Then the physical insight could suggest (incorrectly) that the larger of the two particles depicted in Figure 4 would experience larger capillary force, as far as the capillary force is an integral of distributed forces (pressure through the particle surface and surface tension along the contact line, cf. eqs 1.4–1.6). Indeed, the hydrostatic pressure and surface tension contributions to the lateral capillary force, separately, can be different:

$$\mathbf{F}^{(1p)} \neq -\mathbf{F}^{(2p)}; \qquad \mathbf{F}^{(1\gamma)} \neq -\mathbf{F}^{(2\gamma)} \tag{2.1}$$

Nevertheless, it turns out that an analogue of Newton's third law, eq 1.7, holds for the *total* capillary force, as defined by eq 1.4. The validity of eq 1.7 was proven in ref 14 under the following restrictions: (i) small meniscus slope, i.e. eq 1.18 holds; (ii) constant contact angle at the particle surface; (iii) the derivation is exact for vertical circular cylinders and approximate for spherical particles.

Below we present a general proof of eq 1.7, which is not subjected to restrictions i–iii. The hydrostatic pressure and surface tension contributions to the capillary force will be considered separately.

Hydrostatic Pressure Contribution. If the meniscus shape is determined by eq 1.8, the hydrostatic pressure can be written in the form

$$\bar{P} = P_I(z)\theta(\zeta(x,y) - z) + P_{II}(z)\theta(z - \zeta(x,y)) \tag{2.2}$$

where P_I and P_{II} are determined by eq 1.3 and

$$\theta(x) = 0 \text{ for } x < 0$$
$$= 1 \text{ for } x > 0 \tag{2.3}$$

is the Heaviside stepwise function. As known[25]

$$\frac{d}{dx}\theta(x) = \delta(x) \tag{2.4}$$

where $\delta(x)$ is the Dirac function. From eq 1.6 one obtains

$$\sum_{k=1}^{2}\mathbf{F}^{(kp)} = -\sum_{k=1}^{2}\oint_{S_k} d\mathbf{s}\cdot(\mathbf{U}_{II}\bar{P}) = \int_{V_{out}} dV\mathbf{U}_{II}\cdot\nabla\bar{P} \tag{2.5}$$

At the last step we used the Gauss theorem with V_{out} being the volume outside the two particles; when the "particles" are two infinitely long cylinders, S_1 and S_2 are their lateral surfaces and the meaning of V_{out} remains the same. From eqs 2.2 and 2.4 one derives

$$\mathbf{U}_{II}\cdot\nabla\bar{P} = \nabla_{II}\bar{P} = [P_I(\zeta) - P_{II}(\zeta)]\delta(z - \zeta(x,y))\nabla_{II}\zeta \tag{2.6}$$

Then eqs 2.5 and 2.6 yield

$$\sum_{k=1}^{2}\mathbf{F}^{(kp)} = \int_{S_0} ds[P_I(\zeta) - P_{II}(\zeta)]\nabla_{II}\zeta \tag{2.7}$$

where the integral is taken over this part of the plane xy, which represents orthogonal projection of the liquid meniscus.

Surface Tension Contribution. From eq 1.5 one obtains

$$\sum_{k=1}^{2}\mathbf{F}^{(k\gamma)} = \mathbf{U}_{II}\cdot\sum_{k=1}^{2}\oint_{L_k} d\mathbf{l}\mathbf{u}\gamma \tag{2.8}$$

Then one can apply the Green–Gauss–Ostrodradsky theorem in the form[26,27]

$$\oint_C d\mathbf{l}\mathbf{u}\varphi = \int_S ds(\tilde{\nabla}_{II}\varphi + 2H\tilde{\mathbf{n}}\varphi) \tag{2.9}$$

where φ is a scalar, S is a part of a curved surface encompassed by the contour C; H, $\tilde{\mathbf{n}}$, and ∇_{II} are the mean curvature, the running unit normal and the two-dimensional gradient operator of surface S. In our case S is the meniscus surface, whose boundaries are the two contact lines, L_1 and L_2, taken with negative orientation, and $\varphi \equiv \gamma = \text{const}$. Then from eqs 2.8–2.9 one derives

$$\sum_{k=1}^{2}\mathbf{F}^{(k\gamma)} = -\mathbf{U}_{II}\cdot\int_S ds2H\tilde{\mathbf{n}}\gamma \tag{2.10}$$

The position vector of a point of meniscus surface S is

$$\mathbf{R}(x,y) = x\mathbf{e}_x + y\mathbf{e}_y + \zeta(x,y)\mathbf{e}_z \tag{2.11}$$

where $\mathbf{e}_x$, $\mathbf{e}_y$, and $\mathbf{e}_z$ are the unit vectors of the Cartesian coordinate axes. Then

$$\mathbf{a}_x = \frac{\partial\mathbf{R}}{\partial x} \text{ and } \mathbf{a}_y = \frac{\partial\mathbf{R}}{\partial y} \tag{2.12}$$

are the vectors of a local basis in S and hence the unit normal $\tilde{\mathbf{n}}$ can be represented in the form

(25) Korn, G. A.; Korn, T. M. *Mathematical Handbook*; McGraw-Hill: New York, 1968.
(26) Brand, L. *Vector and Tensor Analysis*; Wiley: New York, 1947.
(27) Weatherburn, C. E. *Differential Geometry of Three Dimensions*; University Press: Cambridge, 1939.

Table I. List of Available Analytical Expressions for the Lateral Capillary Force at Various Configurations

configuration	boundary condition	reference
two horizontal cylinders (flotation force)	fixed contact angle	ref 12
two vertical cylinders (immersion force)	fixed contact angle	refs 3 and 14
	fixed contact line	this paper, eq 1.24
two spheres (flotation force)	fixed contact angle	refs 12 and 16, this paper, eq 5.4
two spheres or sphere/vertical cylinder (immersion force)	fixed contact angle	refs 3 and 14
wall/vertical cylinder wall/sphere (immersion force)	fixed contact angle	ref 15

$$\tilde{\mathbf{n}} = (\mathbf{a}_x \times \mathbf{a}_y)/|\mathbf{a}_x \times \mathbf{a}_y| \tag{2.13}$$

From eqs 2.11–2.13 one derives

$$\tilde{\mathbf{n}} = (\mathbf{e}_z - \nabla_{II}\zeta)/(1 + |\nabla_{II}\zeta|^2)^{1/2} \tag{2.14}$$

where ∇_{II} is defined by eq 1.11. Then

$$ds\mathbf{U}_{II}\cdot\tilde{\mathbf{n}} = \frac{ds}{(1 + |\nabla_{II}\zeta|^2)^{1/2}}(-\nabla_{II}\zeta) = -dx\,dy\,\nabla_{II}\zeta \tag{2.15}$$

and hence the integral in eq 2.10 can be taken over the projection, S_0, of surface S in the plane xy

$$\sum_{k=1}^{2}\mathbf{F}^{(k\gamma)} = \int_{S_0} ds 2H\gamma\nabla_{II}\zeta \tag{2.16}$$

Finally, from eqs 1.4, 1.9, 2.7, and 2.16 one obtains

$$\mathbf{F}^{(1)} + \mathbf{F}^{(2)} = \int_{S_0}[2H\gamma + P_I(\zeta) - P_{II}(\zeta)]\nabla_{II}\zeta = 0 \tag{2.17}$$

i.e. we established the validity of eq 1.7. Equation 2.17 is a consequence only of the fact that the meniscus shape obeys the Laplace equation, eq 1.9, irrespective of the boundary conditions at the contact line (constant contact angle, constant elevation, or something else). Note also that during the derivation of eq 2.17 we did not use any assumptions to specify the shape of the two interacting particles. A straightforward generalization of eq 2.17 is possible for N interacting particles

$$\sum_{k=1}^{N}\mathbf{F}^{(k)} = 0 \tag{2.18}$$

One effect which is not taken into account in the derivation of eq 2.17 is the disjoining pressure, which appears when the liquid layer (see Figure 2b,d,e) is thin enough. This effect is considered in the next section.

Newton's Third Law for Capillary Forces: Thin Films

The disjoining pressure, Π, represents the surface force per unit area of the thin film surface. Π can be due to van der Waals, double layer, hydrophobic, solvation, steric, etc. surface forces.[28,29] From a thermodynamic viewpoint the disjoining pressure is an excess pressure, which appears, when the real thin liquid film (of nonuniform density and nonisotropic pressure tensor) is described theoretically as an idealized liquid layer of uniform density and isotropic pressure, P_I, sandwiched between two mathematical Gibbsean dividing surfaces. To make this idealized liquid layer mechanically equivalent to the real thin film, one introduces in the idealized system an additional pressure, the disjoining pressure, coupled with a variable film surface tension, which depends on the film thickness.[30,31]

When particles are confined in an initially plane-parallel thin liquid film (see Figures 2, 4, and 5), they create deformation of its surfaces, i.e. we have to deal with films of *uneven* thickness. In this case the overall shape of the liquid film is characterized by the so-called "reference surface", which is located somewhere inside the film.[31] For example, the reference surface of the film depicted in Figure 3f is its midplane; in a spherical, vesiclelike film the reference surface will be spherical, etc. Then the disjoining pressure, Π, is a vectorial quantity representing the excess force per unit area of this reference surface (see eq 3.12 in ref 31). The generalization of the Laplace equation, 1.9, for the film surface (cf. eq 3.16 in ref 31) reads

$$\tilde{\nabla}_{II}\cdot\tilde{\mathbf{T}} + [P_I(\zeta) - P_{II}(\zeta)]\tilde{\mathbf{n}} + c\Pi = 0 \tag{3.1}$$

Here ζ is the distance between a point of the film surface and the reference surface; $\tilde{\mathbf{n}}$ and $\tilde{\nabla}_{II}$ have the same meaning as in eq 2.9 referring to the film surface; c is a geometrical coefficient determined by eq 3.20 in ref 31; $\tilde{\mathbf{T}}$ is the film surface stress tensor. When the interfacial curvature effects are negligible, $\tilde{\mathbf{T}}$ is an isotropic surface tensor:

$$\tilde{\mathbf{T}} = \gamma\tilde{\mathbf{U}}_{II} \tag{3.2}$$

with $\tilde{\mathbf{U}}_{II}$ being the two-dimensional unit tensor in the film surface and γ being the film surface tension. In the limiting case of a thick film $\Pi = 0$, γ = const and by using the identity[32]

$$\tilde{\nabla}_{II}\cdot\tilde{\mathbf{U}}_{II} = 2H\tilde{\mathbf{n}} \tag{3.3}$$

form eqs 3.1 and 3.2 one recovers the Laplace equation 1.9. For our considerations below it is not necessary to specify some explicit expression for $\tilde{\mathbf{T}}$; we need only the following general property of $\tilde{\mathbf{T}}$:

$$\tilde{\mathbf{n}}\cdot\tilde{\mathbf{T}} = 0 \tag{3.4}$$

cf. eq 2.12 in ref 31. Besides, the equivalence between the real and idealized systems with respect to the forst moments implies that the disjoining pressure is perpendicular to the reference surface:

$$\mathbf{U}_{II}\cdot\Pi = 0 \tag{3.5}$$

Here and hereafter in this section $\mathbf{U}_{II}$ is the idemfactor (unit tensor) of the reference surface. (Equation 3.4 is derived in ref 31 for the special case of planar reference surface. However, a closer inspection of eq 3.30 in ref 31 shows that one can set $\tilde{\mathbf{R}} = 0$ and then eq 3.5 above is obtained as a general result if some negligible gravitational terms are omitted.) Below for the sake of simplicity we suppose that the reference surface is planar.

Equations 2.5, 2.7, and 2.14 above, originally derived for a thick film ($\Pi = 0$), are applicable also for a thin film ($\Pi \neq 0$) with U_{II} and ∇_{II} being operators in the reference surface. In particular, from eqs 2.7 and 2.14 one derives

(28) Derjaguin, B. V. *Stability of Colloids and Thin Liquid Films*; Plenum Press, Consultants Bureau: New York, 1989.
(29) Israelachvili, J. *Intermolecular and Surface Forces*, 2nd ed.; Academic Press: London, 1992.
(30) Kralchevsky, P. A.; Ivanov, I. B. *Chem. Phys. Lett.* **1985**, *121*, 116.
(31) Kralchevsky, P. A.; Ivanov, I. B. *J Colloid Interface Sci.* **1990**, *137*, 234.
(32) Aris, R. *Vectors, Tensors and the Basic Equations of Fluid Mechanics*; Prentice Hall: New York, 1962.

$$\sum_{k=1}^{2}\mathbf{F}^{(kp)} = -\mathbf{U}_{\Pi}\cdot\int_S ds\tilde{\mathbf{n}}[P_I(\zeta) - P_{II}(\zeta)] \qquad (3.6)$$

where S denotes the film surface. On the other hand, in the case of thin films the definition 1.5 can be generalized as follows:

$$\mathbf{F}^{(k\gamma)} = \mathbf{U}_{\Pi}\cdot\oint_{L_k} dl(\mathbf{u}\cdot\tilde{\mathbf{T}})$$

Then one can use a modified version

$$\oint_C dl\mathbf{u}\cdot\mathbf{T} = \int_S ds(\tilde{\nabla}_{\Pi}\cdot\mathbf{T} + 2H\tilde{\mathbf{n}}\cdot\mathbf{T}) \qquad (3.7)$$

of the Green–Gauss–Ostrogradsky theorem, eq 2.9, with $\mathbf{T}$ being an arbitrary tensor, to obtain

$$\sum_{k=1}^{2}\mathbf{F}^{(k\gamma)} = -\mathbf{U}_{\Pi}\cdot\int_S ds\tilde{\nabla}_{\Pi}\cdot\tilde{\mathbf{T}} \qquad (3.8)$$

At the last step eq 3.4 was utilized. A combination of eqs 1.4, 3.1, 3.5, 3.6, and 3.8 finally yields

$$\mathbf{F}^{(1)} + \mathbf{F}^{(2)} = -\mathbf{U}_{\Pi}\cdot\int_S ds\{\tilde{\nabla}_{\Pi}\cdot\tilde{\mathbf{T}} + [P_I(\zeta) - P_{II}(\zeta)]\tilde{\mathbf{n}} + c\Pi\} = 0 \qquad (3.9)$$

i.e. we arrived again at eq 1.7. Hence, an analogue of Newton's third law holds also for the capillary forces between particles confined in a thin liquid film.

Equivalence between the Energetical and Force Approaches

Our purpose here is to demonstrate a variational method for proving that the energetical and force approaches to the lateral capillary forces are equivalent. We consider a configuration of simpler geometry, when the two interacting "particles" are two vertical cylinders, not necessarily circular. This can be the case of a single interface, depicted in Figure 3, or the case of two interfaces (thin liquid film) shown in Figure 5c. In the latter case the disjoining pressure effect (the interaction between the two film surfaces) becomes important. For the sake of simplicity we consider a symmetrical film of planar reference surface (Figure 5c) and we will deal with the upper film surface, the treatment of the lower film surface being analogous.

Our starting point is eq 1.1, which represents the basis of the energetical approach. For the geometry of consideration the different terms in eq 1.1 can be specified as follows:

$$A = \int_{S_0} ds(1 + \zeta_x^2 + \zeta_y^2)^{1/2} \qquad (4.1)$$

$$\int_{V_I} P_I\, dV = \int_{S_0} ds\int_{z_1}^{\zeta} dz P_I \qquad (4.2)$$

$$\int_{V_{II}} P_{II}\, dV = \int_{S_0} ds\int_{\zeta}^{z_2} dz P_{II} \qquad (4.3)$$

$$A_{k,I} = \oint_{C_k} dl\int_{z_1}^{\zeta} dz,\ A_{k,II} = \oint_{C_k} dl\int_{\zeta}^{z_2} dz \qquad (4.4)$$

For the sake of brevity we use the notation

$$\zeta_x = \frac{\partial\zeta}{\partial x}, \qquad \zeta_y = \frac{\partial\zeta}{\partial y} \qquad (4.5)$$

S_0 has the same meaning as in eq 2.7. It is assumed that the system under consideration is situated between the planes $z = z_1$ and $z = z_2$, located on the two opposite sides of the interface $z = \zeta(x,y)$. These two planes play an auxiliary role: the final results do not depend on the choice of z_1 and z_2. That is why the exact location of z_1 and z_2 is not important. C_k ($k = 1, 2$) is a contour representing the orthogonal projection of contact line L_k onto plane xy.

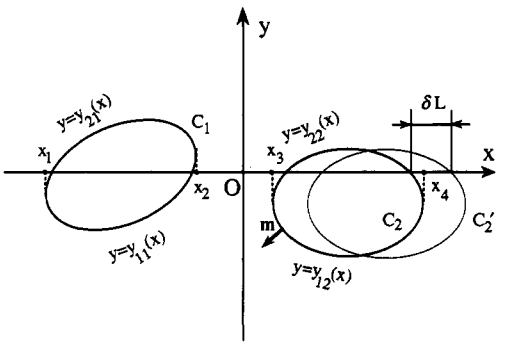

Figure 8. Sketch of the contours C_1 and C_2 representing the horizontal projections of the lateral surfaces of the vertical cylinders 1 and 2; C_2' is the position of C_2 after the displacement.

As far as the two cylinders are not allowed to move along the vertical, the first term in the right-hand side of eq 1.1 is constant an can be omitted. Then eqs 1.1 and 4.1–4.5 yield

$$\Omega = \int_{S_0} ds\Phi(\zeta,\zeta_x,\zeta_y) + \sum_{k=1}^{2}\oint_{C_k} dl[\omega_{k,I}(\zeta - z_1) + \omega_{k,II}(z_2 - \zeta)] \qquad (4.6)$$

where

$$\Phi = -\int_{z_1}^{\zeta} dz P_I - \int_{\zeta}^{z_2} dz P_{II} + \gamma(1 + \zeta_x^2 + \zeta_y^2)^{1/2} \qquad (4.7)$$

Equations 4.6 and 4.7 hold for both thick film ($\Pi = 0$) and thin film ($\Pi \neq 0$). Nevertheless, there are some implicit differences in the formalism in these two cases:

(i) In the case of *thick* film (single interface) γ = const and ζ satisfies the conventional Laplace equation, eq 1.9.

(ii) In the case of *thin* film the surface tension depends on the local film thickness;[30,31] as far as l_0 is fixed (Figure 5c) one has $\gamma = \gamma(\zeta)$. The latter dependence is determined by the equation (see Appendix II)

$$\frac{d\gamma}{d\zeta} = -(1 + |\nabla_{\Pi}\zeta|^2)^{-1/2}\Pi \qquad (4.8)$$

In addition, the shape of the film surface satisfies the following generalized version of the Laplace equation (see Appendix II):

$$2H\gamma = (P_{II} - P_I)_{z=\zeta} - (1 + |\nabla_{\Pi}\zeta|^2)^{-1}\Pi \qquad (4.9)$$

One can easily check that when $\Pi \to 0$ eqs 4.8 and 4.9 yield the respective results for a thick film.

Let us now consider an infinitesimal displacement, δL, of cylinder 2 along axis x. Consequently, contour C_2 will be displaced in a new position, C'_2; see Figure 8. By using Laplace and Neumann–Young equations, in conjunction with some methods of the variational calculus,[33] one derives the following expression for the variation of Ω (see Appendix III)

$$\frac{\delta\Omega}{\delta L} = -\mathbf{e}_x\cdot\mathbf{F}^{(2p)} - \oint_{C_2} dl\gamma\left[(1 + \zeta_x^2 + \zeta_y^2)^{1/2}\frac{dy}{dl} + \zeta_x\mathbf{m}\cdot\tilde{\mathbf{n}}\right] \qquad (4.10)$$

where in view of eqs 1.6 and 2.2

(33) Elsgoltz, L. E. *Differential Equations and Variational Calculus*; Nauka: Moscow, 1969; in Russian.

$$\mathbf{F}^{(2p)} = \oint_{C_2} dl \int_{z_1}^{z_2} dz(-\mathbf{m}\bar{P}) \tag{4.11}$$

is the hydrostatic pressure contribution to the lateral capillary force and the expression

$$\mathbf{m} = \frac{dy}{dl}\mathbf{e}_x - \frac{dx}{dl}\mathbf{e}_y \tag{4.12}$$

defines the outer unit normal to contour C_2, shown in Figure 8. By using eqs 2.14 and 4.12 one can derive

$$(1 + \zeta_x^2 + \zeta_y^2)^{1/2}\frac{dy}{dl} + \zeta_x \mathbf{m}\cdot\tilde{\mathbf{n}} = (1 + |\nabla_{II}\zeta|^2)^{-1/2}\left(\zeta_y\frac{d\zeta}{dl} + \frac{dy}{dl}\right) \tag{4.13}$$

On the other hand, at each point of the three-phase contact line L_2 one has:

$$\mathbf{u} = \mathbf{t} \times \tilde{\mathbf{n}} \tag{4.14}$$

where $\mathbf{t}$ is the running unit tangent to L_2 and the meaning of $\mathbf{u}$ is the same as in eq 1.5. The running position vector of a point on L_2 can be expressed in the form

$$\mathbf{R}(\tilde{l}) = x(\tilde{l})\mathbf{e}_x + y(\tilde{l})\mathbf{e}_y + \zeta(\tilde{l})\mathbf{e}_z \tag{4.15}$$

where $\tilde{l}$ is the natural parameter (the length) along L_2. Then

$$\mathbf{t} \equiv \frac{d\mathbf{R}}{d\tilde{l}} = \frac{dx}{d\tilde{l}}\mathbf{e}_x + \frac{dy}{d\tilde{l}}\mathbf{e}_y + \frac{d\zeta}{d\tilde{l}}\mathbf{e}_z \tag{4.16}$$

From eqs 2.14, 4.14, and 4.16 it follows

$$\mathbf{e}_x\cdot\mathbf{u} = (1 + |\nabla_{II}\zeta|^2)^{-1/2}\left(\zeta_y\frac{d\zeta}{dl} + \frac{dy}{dl}\right)\frac{dl}{d\tilde{l}} \tag{4.17}$$

with dl being the elementary length along contour C_2. Finally, by means of eqs 4.13 and 4.17 one can represent eq 4.10 in the form

$$\frac{\delta\Omega}{\delta L} = -\mathbf{e}_x\cdot[\mathbf{F}^{(2p)} + \mathbf{F}^{(2\gamma)}] \tag{4.18}$$

where

$$\mathbf{F}^{(2\gamma)} = \mathbf{U}_{II}\cdot\oint_{L_2} d\tilde{l}\,\mathbf{u}\gamma \tag{4.19}$$

Equation 4.18 along with eqs 4.11 and 4.19 gives a proof of the equivalence between the energetical approach, based on eq 1.1, and the force approach, based on eqs 1.4–1.6. We hope the variational method presented above can be extended to particles of general shape.

Numerical Results and Discussion

In this section we focus our attention on lateral capillary forces between colloidal particles in *thin* films; see Figures 2b, 2f, and 5c. The intriguing point is how large is the effect of disjoining pressure on the magnitude of the capillary interaction. The disjoining pressure becomes significant when the thickness, h, of the liquid film is small enough. On that reason the calculations presented below are carried out with comparatively thin films ($h \leq 20$ nm). The thermodynamic (macroscopic) disjoining pressure approach has been proven to give an adequate description of the properties of such films.[28,29] Therefore, we hope the theory presented in the previous sections, which is based on the disjoining pressure approach, is appropriate enough to allow a correct numerical estimate of the capillary interactions in thin films.

We consider two model examples. The first of them is related to the conditions of the experiments by Yoshimura *et al.*[4,5] with globular proteins in thin aqueous films on mercury substrate. The second example models the interaction of membrane proteins incorporated in a phospholipid bilayer in water environment; see, e.g., ref 29.

Table II. Capillary Length q^{-1} vs Film Thickness, h, for the Water–Gas Surface of an Aqueous Film on Hg (A_H = -7.22×10^{-20} J, γ = 72 mN/m)

h, nm	q^{-1}, nm	h, nm	q^{-1}, nm
5.0	63	15.0	563
7.5	141	17.5	767
10.5	250	20.0	1001
12.5	391		

Spherical Particles in Aqueous Film on Mercury. We suppose that the aqueous solution spread on mercury contains electrolyte with concentration high enough to suppress the electrostatic double layer interaction. If such is the case, the stability of the aqueous thin film is ensured by the *repulsive* van der Waals disjoining pressure[34]:

$$\Pi(h) = \Pi_{VW}(h) \equiv -\frac{A_H}{6\pi h^3} \tag{5.1}$$

The Hamaker constant for this system was estimated by Usui *et al.*[34] to be $A_H = -7.22 \times 10^{-20}$ J. Then the surface tension of the boundary between aqueous film and air is[35]

$$\gamma(h) = \gamma_0 + \frac{1}{2}\int_h^\infty \Pi(h)\,dh = \gamma_0 - \frac{A_H}{24\pi h^2} \tag{5.2}$$

where γ_0 is the surface tension of a thick film ($h \to \infty$). For $h \geq 5$ nm one calculates $|A_H|/(24\pi h^2) \leq 3.8 \times 10^{-2}$ mN/m. Hence, in our calculations we can neglect the dependence of γ on h; i.e. we can set $\gamma \approx \gamma_0$ = const. On the same reason the contact angle α, formed at the particle/water/gas contact line, can be considered (approximately) as being independent of h.

Since the surface tension of the boundary between mercury and water is rather high ($\gamma_{MW} \approx 470$ mN/m) in our estimates below we will neglect the deformation of the mercury surface due to the presence of particles and we will account only for the deformation of the water–gas interface; cf., e.g., Figure 2b.

From eq 5.1 one obtains

$$\Pi' = \frac{A_H}{2\pi h^4} \tag{5.3}$$

From eqs 1.17 and 5.3 we calculated the capillary length, q^{-1}, for the water–gas interface; γ = 72 mN/m was used for the surface tension. The results shown in Table II demonstrate a strong dependence of the capillary length on the film thickness. q^{-1} is smaller when the film is thinner and the repulsive disjoining pressure is higher. The disjoining pressure tends to keep the film surface planar and to suppress the capillary waves or any other surface deformation. In this aspect it behaves similarly to the gravity force but is much stronger. (For example, the capillary length due to gravity, calculated from eq 1.12, is q^{-1} = 2.7 mm on the Earth and q^{-1} = 1.6 mm on Jupiter; compare the latter values with those in Table II.)

As far as eq 1.1 is applicable for both thick and thin films, we will use a procedure, which is analogous to that developed in ref 3 for calculating the free energy of capillary interaction, $\Delta\Omega$, between two identical spherical particles, which are partially immersed in the film. According to this procedure

(34) Usui, S.; Sasaki, S.; Hasegawa, F. *Colloids Surf.* **1986**, *18*, 53.
(35) Ivanov, I. B.; Toshev, B. V. *Colloid Polym. Sci.* **1975**, *253*, 593.

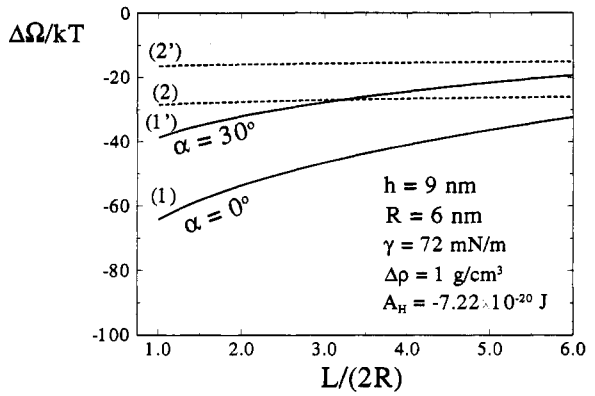

Figure 9. Capillary interaction energy $\Delta\Omega$ vs distance L between two identical spherical particles of radius R in a thin aqueous film on a mercury substrate. Curves 2 and 2′ are calculated at "switched off" disjoining pressure ($\Pi = 0$), whereas $\Pi \neq 0$ for curves 1 and 1′. h is the thickness of the plane-parallel film far from the particles, γ is the meniscus surface tension, $\Delta\rho$ is the difference between the mass densities of the film phase (water) and the upper phase (gas), and A_H is the Hamaker constant for an aqueous film sandwiched between mercury and gas.

$$\Delta\Omega = -2\pi\gamma_0(A_1 - A_\infty) \tag{5.4}$$

where

$$A_1 = 2h_cR\cos\alpha - h_cr_c\sin\Psi_c + r_c^2$$

$$A_\infty = 2h_{c\infty}R\cos\alpha - h_{c\infty}r_{c\infty}\sin\Psi_{c\infty} + r_{c\infty}^2$$

As usual, R is particle radius and the subscript "∞" denotes the value of respective parameter for infinite interparticle separation ($L \to \infty$). The distance between the three-phase contact line and the substrate surface is

$$l = h + h_c \tag{5.5}$$

Additional simple geometrical considerations yield

$$r_c = [(2R - l)l]^{1/2} \tag{5.6}$$

$$\Psi_c = \arcsin\frac{r_c}{R} - \alpha \tag{5.7}$$

Then at given film thickness h, contact angle α, and interparticle distance L the six unknown geometrical parameters, h_c, r_c, Ψ_c, l, a, and τ_c can be determined from the set of six equations, eqs 1.21–1.23 and 5.5–5.7. The limiting values for $L \to \infty$ are similarly determined from eqs 1.20 and 5.5–5.7, where r_c, Ψ_c, and h_c must be replaced by $r_{c\infty}$, $\Psi_{c\infty}$, and $h_{c\infty}$. Finally the results are substituted in eq 5.4 and $\Delta\Omega$ is calculated.

Curves $\Delta\Omega$ vs L are shown in Figure 9 for $\alpha = 0°$ (curves 1 and 2) and $\alpha = 30°$ (curves 1′ and 2′). To specify the system we chose $R = 6$ nm, $h = 9$ nm (typical values in the experiments with ferritin[4,5]). The disjoining pressure affects $\Delta\Omega$ through the capillary length q^{-1}, which takes part in eqs 1.20 and 1.21. Curves 1 and 1′, are calculated with q determined from eqs 1.17 and 5.3. Curves 2 and 2′ are calculated by setting $\Pi' = 0$ in eq 1.17; i.e. these curves correspond to an imaginary film in which the disjoining pressure is "switched off". The area confined between curves 1 and 2 (or 1′ and 2′) visualizes the effect of disjoining pressure on the capillary interaction energy $\Delta\Omega$. One sees that the latter effect is important and comparable by magnitude with the contact angle effect.

The fact that the capillary interaction between the particles of smaller contact angle is stronger is due to the higher capillary rise of the water along the more hydrophilic particle surface which results in a larger meniscus deformation. In all cases the calculated values of $\Delta\Omega$ are negative (attractive interaction) and many times larger than the thermal energy kT. Hence, this capillary attraction can be the reason for the particle assembly and two-dimensional crystal formation observed experimentally with thin films on substrate.[4,5]

Cylindrical Particles in a Lipid Film. Now we consider the system depicted in Figure 5c. The position of the contact line is fixed at the boundary between the lipophilic and hydrophilic domains of the particle surface. To model a lipid bilayer we choose the thickness of the film, $h = 2l_0$ (Figure 5c) to be 30 Å; see, e.g., ref 29. The disjoining pressure in this system can be written in the form

$$\Pi(h) = \Pi_{VW}(h) + \Pi_{st}(h) \tag{5.8}$$

Here Π_{VW} is the van der Waals disjoining pressure defined by eq 5.1; however the Hamaker constant is now positive (attractive interaction). We specify $A_H = 5\times10^{-21}$ J, which is a typical value for the interaction of aqueous phases across a hydrocarbon film.[29] Π_{st} in eq 5.8 is the steric disjoining pressure, which is caused by the repulsion between the interpenetrating hydrocarbon tails (brushes) of the two attached phospholipid monolayers. Since this situation corresponds to the interaction between two terminally anchored polymer layers in θ-solvent, one can use the expression for the interaction free energy, $f_{st}(h)$, due to Dolan and Edwards[36]

$$f_{st} \equiv \int_h^\infty \Pi_{st}(h)\,dh = 4\Gamma kT\exp\left(-\frac{3h^2}{2\lambda^2}\right) \tag{5.9}$$

$$h^2 > 3\lambda^2$$

Here Γ is the number of polymer chains per unit area of the monolayer and λ has the meaning of root-mean-square end-to-end distance of a chain. For our model calculations we specify $\Gamma^{-1} = 40$ Å^2. To find an estimate of λ consistent with the values of the other parameters we proceed in the following way.

It is natural to suppose that at equilibrium conditions the van der Waals attraction and the steric repulsion counterbalance each other. Then by setting $\Pi = 0$ and $h = 30$ Å in eq 5.8 and by substituting the expressions for Π_{VW} and Π_{st} stemming from eqs 5.1 and 5.9 one calculates $\lambda = 11.5$ Å. With these values of h and λ one obtains $\Pi' = 5.55\times10^{13}$ J/m^4.

The value of the film surface tension γ can vary depending on the experimental conditions; in our model calculations we specify $\gamma = 30$ mN/m. Then eq 1.17 yields a capillary length $q^{-1} = 232.5$ Å. In addition we specify $r_c = 25$ Å, which is in the range of the radii of the membrane proteins. Then if the interparticle separation, L, and contact line elevation, $h_{c\infty}$ (Figure 5c), are known, one can calculate the energy of lateral capillary interaction between the two protein macromolecules as follows: (i) from eq 1.20 one calculates $\Psi_{c\infty}$; (ii) by means of eqs 1.22 and 1.23 one determines a and τ_c; (iii) by using eqs A.8 and A.12 (Appendix I) one calculates $\sin\Psi_c(L)$; (iv) a substitution of the parameters thus determined into eq 1.24 yields the capillary interaction energy. Note that there are *two* deformed liquid surfaces in the case of symmetrical thin film (Figure 5c) and hence the interaction energy $\Delta\Omega$ (listed in Table III) is *twice* the interaction energy as given by eq 1.24.

(36) Dolan, A. K.; Edwards, S. F. *Proc. R. Soc. London* **1975**, *A343*, 627.

Table III. Dependence of the Capillary Interaction Energy $\Delta\Omega$ on the Distance L between the Axes of Two Cylindrical Particles, Figure 5c (r_c = 25 Å, γ = 30 mN/m, T = 298 K, q^{-1} 232.5 Å)

	$-\Delta\Omega/\kappa T$	
L/r_c	$h_{c\infty}$ = 4 Å	$h_{c\infty}$ = 8 Å
2.0	2.38	9.54
2.5	2.22	8.88
3.0	2.06	8.22
3.5	1.90	7.58
4.0	1.74	6.96
4.5	1.58	6.34
5.0	1.44	5.74

The data for $\Delta\Omega$ vs L shown in Table III correspond to two different values of the contact line elevation $h_{c\infty}$. One sees that in spite of the relatively small elevation and particle size, the energy of capillary interaction can be several times kT. In addition, the resulting interparticle attraction appears to be rather long-ranged.

It should be noted, that the range of interaction depends on the value of the film surface tension γ, as far as $q^{-1} \propto \gamma^{1/2}$; cf. eq 1.17. If γ is decreased, then both the range and the magnitude of the capillary attraction will decrease (cf. eq 1.24). On the contrary, at not too low values of γ the lateral capillary forces can be strong enough to create two-dimensional particle aggregation in the film (membrane).

Concluding Remarks

The results of this article can be summarized as follows:

(i) The difference between flotation and immersion lateral capillary forces is demonstrated. The former originates from the particle weight, whereas the latter is engendered by the particle wettability (position of the contact line and magnitude of the contact angle). Both these forces appear when a liquid interface is deformed due to the presence of attached particles. That is the reason why these forces exhibit the same functional dependence on the interparticle distance (see e.g. eqs 1.26 or 1.28). On the other hand, their different physical origin results in different magnitudes of the "capillary charges" of these two kinds of capillary forces (as a rule, the immersion force is much stronger than the flotation force; see Figure 7). In this aspect they resemble the electrostatic and gravitational forces, which obey the same power law, but differ in the physical meaning and magnitude of the force constants (charges, masses).

(ii) In addition to the capillary interactions at fixed contact angle, interactions at fixed contact line (Figure 5) are investigated and respective expressions for the interaction energy are derived (see eqs 1.24 and 1.25 and Appendix I). The numerical test (Figure 6) shows that the capillary interaction at fixed contact angle is stronger than that at fixed contact line.

(iii) A general proof is given to an analogue of Newton's third law for lateral capillary forces between two particles. This proof is valid for both thick ($\Pi = 0$) and thin ($\Pi \neq 0$) films, as well as for both immersion and flotation forces, at general boundary conditions on the particles surfaces.

(iv) The equivalence of the energetical and force approaches to the lateral capillary forces is proven analytically for the special case of two vertical cylinders (not necessarily circular). The proof is valid for both thick and thin films at fixed contact angle or fixed contact line boundary conditions. The equivalency between the energetical and force approaches, as well as Newton's third law for capillary forces, provide useful tests of the numerical results for capillary interactions. Such tests enable one to check the precision of the obtained solution of Laplace equation, eq 1.10, which is a nonlinear partial differential equation and can be solved by using either approximated analytical expansions or sophisticated computer integration procedures.

(v) The effect of disjoining pressure, Π, on the energy of capillary interaction, $\Delta\Omega$, is studied quantitatively in the case of small meniscus slope, when Laplace equation can be linearized. Π affects the capillary interaction through the capillary length, q^{-1}; see Table I. The effect of Π on $\Delta\Omega$ is comparable by magnitude with the contact angle effect; cf. Figure 9. The specified model systems studied quantitatively show that the capillary interactions between particles of nanometer size are strong enough to produce two-dimensional particle aggregation and ordering, as observed experimentally.[4,5,19,20]

Acknowledgment. This work was supported by the Research and Development Corporation of Japan (JRDC) under the program "Exploratory Research for Advanced Technology" (ERATO).

Appendix I. Meniscus Shape at Boundary Condition of Constant Elevation

Our aim is to determine the meniscus shape, $\zeta(x,y)$, in the case when the meniscus elevation at the contact line does not depend on the interparticle separation, L; see Figure 5. Under the restriction for small meniscus slope, eq 1.18, the Laplace equation, eq 1.10, can be linearized to read

$$\nabla_{II}^2 \zeta = q^2 \zeta \qquad \text{(A.1)}$$

To solve eq A.1 along with the boundary conditions, eqs 1.13 and 1.16, we will make use of the mathematical approach developed in ref 3, which is based on the method of the matched asymptotic expansions.[37] This method can be applied when a small parameter is available in the equation. In our case qr_c (or qa) can serve as a small parameter. Then in the region close to the particles (at distances of the order of r_c) and in the region far from the particles (at distances of the order of q^{-1}) asymptotic solutions of eq A.1 are found. Finally, these solutions, called "inner" and "outer" solution,[37] are matched by means of an appropriate procedure; see eq A.9 below. As far as the procedure is analogous to that in ref 3 below, we present only the main steps of the derivation.

Bipolar coordinates (σ,τ) are introduced in the plane xy (see e.g. ref 25):

$$x = \frac{a \sinh \tau}{\cosh \tau - \cos \sigma} \qquad y = \frac{a \sin \sigma}{\cosh \tau - \cos \sigma} \qquad \text{(A.2)}$$

$$-\pi \leq \sigma \leq \pi \qquad -\infty < \tau < +\infty$$

where parameter a is determined by eq 1.22. Each line τ = const is a circumference (see Figure 4 in ref 3). The projections of the two contact lines in the plane xy obey the equations $\tau = \pm\tau_c$, where τ_c is given by eq 1.23. Following the method of the matched asymptotic expansions[37] we introduce an inner and outer region

inner region (close to the cylinders):

$$(\cosh \tau - \cos \sigma)^2 \gg (qa)^2$$

outer region (far from the cylinders):

$$(\cosh \tau - \cos \sigma)^2 \leq (qa)^2$$

In the *inner* region eq A.1 reduces to[3]

(37) Nayfeh, A. H. *Perturbation Methods*; Wiley: New York, 1973.

$$\frac{\partial^2\zeta}{\partial\sigma^2}+\frac{\partial^2\zeta}{\partial\tau^2}=0 \tag{A.3}$$

By using the identity

$$\ln(2\cosh\tau-2\cos\sigma)=|\tau|-\sum_{n=1}^{\infty}\frac{2}{n}\exp(-n|\tau|)\cos n\sigma \tag{A.4}$$

one can check that the expression

$$\zeta^{in}=h_{c\infty}+A\left[\ln(2\cosh\tau-2\cos\sigma)-\tau_c+\sum_{n=1}^{\infty}\frac{2}{n}e^{-n\tau_c}\frac{\cosh n\tau}{\cosh n\tau_c}\cos n\sigma\right] \tag{A.5}$$

satisfies both eq A.3 and the boundary condition 1.16; A is a constant. In the *outer* region eq A.1 reduces to[3]

$$\frac{1}{r}\frac{d}{dr}\left(r\frac{d\zeta}{dr}\right)=q^2\zeta \tag{A.6}$$

From eqs 1.13 and A.6 one derives

$$\zeta^{out}=2AK_0(qr) \tag{A.7}$$

where K_0 is modified Bessel function and constant A is determined by means of the procedure of matching[37]

$$A=h_{c\infty}\left[\tau_c-2\ln(\gamma_e qa)-\sum_{n=1}^{\infty}\frac{2\exp(-n\tau_c)}{n\cosh n\tau_c}\right]^{-1} \tag{A.8}$$

The compound solution for ζ, which is uniformly valid in the inner and outer regions, is[37]

$$\zeta=\zeta^{in}+\zeta^{out}-(\zeta^{out})^{in} \tag{A.9}$$

where

$$(\zeta^{out})^{in}=-2A\ln(\gamma_e qr/2) \tag{A.10}$$

It should be noted that in the boundary regions $\tau\to\pm\tau_c$ or $qr\gg 1$ the inner solution eq A.5 or, respectively, the outer solution, eq A.17, are more accurate than the compound solution, eq A.9.

Angle $\Psi_c(L)$, which appears in eq 1.24, is in fact an average slope angle, defined as follows (see eqs 2.18 and 3.13 in ref 3)

$$h_{c\infty}\sin\Psi_c(L)=\frac{1}{2\pi r_c}\oint_{C_1}dl\,\mathbf{m}\cdot(\zeta\nabla_{II}\zeta) \tag{A.11}$$

where contour C_1 represents the projection of the contact line in the plane xy and $\mathbf{m}$ is running unit normal. From eqs 1.16, A.2, A.5 and A.11 one obtains

$$\sin\Psi_c(L)=\frac{1}{2\pi r_c}\int_{-\pi}^{+\pi}d\sigma\frac{\partial\zeta^{in}}{\partial\tau}\Big|_{\tau=\tau_c}=\frac{A}{r_c} \tag{A.12}$$

$$(qa)^2\ll 1$$

where A is given by eq A.8. For small separation between cylinders surfaces $a\to 0$ (cf. eq 1.22); then $\tau_c\to a/r_c$ and

$$\sum_{n=1}^{\infty}\frac{\exp(-n\tau_c)}{\cosh n\tau_c}\to 2\int_{2\tau_c}^{\infty}\frac{dx}{x(e^x+1)}\to-\ln\frac{4\gamma_e a}{\pi r_c} \tag{A.13}$$

At the last step we have used integration by parts along with the identity[38]

(38) Prudnikov, A. P.; Brychkov, Y. A.; Marichev, O. I. *Integrals and Series*; Nauka: Moscow, 1981; in Russian.

$$\int_0^{\infty}\frac{e^x\ln x}{(e^x+1)^2}dx=\frac{1}{2}\ln\left(\frac{\pi}{2\gamma_e}\right) \tag{A.14}$$

Hence in the limit of close contact ($a\to 0$) the two logarithmically divergent terms in eq A.8 cancel each other and parameter A (and the slope angle Ψ_c) have finite value.

In the other limit, $(qa)^2\gg 1$, one can find expression for $\Psi_c(L)$ by using the superposition approximation.[10,12,14,16] In the framework of this approximation the elevation h_c of the contact line can be presented in the form

$$h_c=h_{c\infty}+\Delta h_c+\left(\frac{\partial h_c}{\partial\sin\Psi_c}\right)_{r_c}(\sin\Psi_c-\sin\Psi_{c\infty}) \tag{A.15}$$

Here $h_{c\infty}$ is the elevation at $L\to\infty$

$$\Delta h_c=r_c\sin\Psi_{c\infty}K_0(qL) \tag{A.16}$$

is the elevation created by a single vertical cylinder at a distance L from its axis (the distance at which the second cylinder is situated); the last term in eq A.15 accounts for the change in h_c due to the change in Ψ_c. From Derjaguin's formula, eq 1.20, one obtains

$$\left(\frac{\partial h_c}{\partial\sin\Psi_c}\right)_{r_c}=r_c\ln\frac{2}{\gamma_e qr_c} \tag{A.17}$$

The boundary condition, eq 1.16, requires $h_c=h_{c\infty}$ and then eqs A.15–A.17 yield the sought for asymptotic expression for $\Psi_c(L)$

$$\sin\Psi_c(L)=\sin\Psi_{c\infty}\left[1-\left(\ln\frac{2}{\gamma_e qr_c}\right)^{-1}K_0(qL)\right] \tag{A.18}$$

Equation A.18 holds when the second term in the brackets is small, i.e. when

$$\epsilon(L)\equiv\left(\ln\frac{2}{\gamma_e qr_c}\right)^{-1}K_0(qL)\ll 1 \tag{A.19}$$

The two asymptotics given by eqs A.12 and A.18 can be matched by applying the standard procedure (cf. eq A.9) to the function $1/\sin\Psi_c(L)$. The resulting compound expression is eq 1.25 above. We recommend to the reader to use eq A.18 when $\epsilon(L)\ll 1$ and to use eq 1.25 in all other cases.

Appendix II. Relationship between Surface Tension and Disjoining Pressure of Thin Liquid Films

When the reference surface of the film is planar the geometrical factor c in eq 3.1 reads (cf. eqs 3.16, 3.20 and 4.3 in ref 31)

$$c=\mathbf{n}\cdot\tilde{\mathbf{n}}=(1+|\nabla_{II}\zeta|^2)^{-1/2} \tag{B.1}$$

where $\mathbf{n}$ and $\tilde{\mathbf{n}}$ are the running unit normals of the reference and upper film surface, respectively. Besides, eq 3.5 means that the vector of disjoining pressure is directed along $\mathbf{n}$. Then one obtains

$$\Pi\cdot\tilde{\mathbf{n}}=\Pi\mathbf{n}\cdot\tilde{\mathbf{n}} \tag{B.2}$$

In addition, eqs 3.2 and 3.3 lead to

$$\tilde{\nabla}_{II}\cdot\tilde{\mathbf{T}}=\tilde{\nabla}_{II}\gamma+2H\gamma\tilde{\mathbf{n}} \tag{B.3}$$

From eqs B.1–B.3 it follows that the projection of the vectorial expression eq 3.1 along the normal $\tilde{\mathbf{n}}$ is in fact eq 4.9. Similarly one can derive that the projection of eq 3.1 in a plane perpendicular to $\tilde{\mathbf{n}}$ reads

$$\tilde{\nabla}_{II}\gamma\equiv\frac{d\gamma}{d\zeta}\tilde{\nabla}_{II}\zeta=-c\Pi\mathbf{n}\cdot\tilde{\mathbf{U}}_{II} \tag{B.4}$$

Let u^α, $\alpha=1,2$, be curvilinear coordinates and $\mathbf{a}_\alpha$ be the respective local basis vectors in the plane of the reference

surface. Then one can prove (cf. eq 2.19 in ref 31) that the vectors

$$\tilde{\mathbf{a}}_\alpha = \mathbf{a}_\alpha + \mathbf{n}\frac{\partial \zeta}{\partial u^\alpha}, \qquad \alpha = 1, 2 \tag{B.5}$$

form a covariant local basis on the film surface. Hence one can write[27,39]

$$\tilde{\nabla}_{\mathrm{II}}\zeta = \tilde{\mathbf{a}}_\beta \tilde{a}^{\beta\alpha}\frac{\partial \zeta}{\partial u^\alpha}, \qquad \tilde{\mathbf{U}}_{\mathrm{II}} = \tilde{\mathbf{a}}_\alpha \tilde{\mathbf{a}}_\beta \tilde{a}^{\alpha\beta} \tag{B.6}$$

where $\tilde{a}^{\alpha\beta} = \tilde{a}^{\beta\alpha}$ are the contravariant components of the film surface metric tensor and summation over the repeating indices is supposed. From eqs B.5 and B.6 one obtains

$$\mathbf{n}\cdot\tilde{\mathbf{U}}_{\mathrm{II}} = \frac{\partial \zeta}{\partial u^\alpha}\tilde{\mathbf{a}}_\beta \tilde{a}^{\alpha\beta} = \tilde{\nabla}_{\mathrm{II}}\zeta \tag{B.7}$$

Having in mind eq B.7 one can transform eq B.4 to read

$$\left(\frac{d\gamma}{d\zeta} + c\Pi\right)\tilde{\nabla}_{\mathrm{II}}\zeta = 0 \tag{B.8}$$

Since in general $\tilde{\nabla}_{\mathrm{II}}\zeta \neq 0$, from eqs B.1 and B.8 one derives the sought for eq 4.8.

Appendix III. Derivation of Equation 4.10

The surface integral in eq 4.6 can be transformed to read

$$\int_{S_0} ds\Phi = \int_{-\infty}^{+\infty} dx\left[\int_{-\infty}^{y_1(x)} dy\Phi + \int_{y_2(x)}^{+\infty} dy\Phi\right] \tag{C.1}$$

where

$$\begin{aligned} y_k(x) &= y_{k1}(x) \quad \text{for } x_1 < x < x_2 \\ &= y_{k2}(x) \quad \text{for } x_3 < x < x_4 \\ &= 0 \quad \text{for all other values of } x \end{aligned} \tag{C.2}$$

points $x_1, \ldots, x_4$ and functions $y_{ik}(x)$, $i,k = 1,2$, are shown in Figure 8. Then the variation of the surface integral induced by the displacement δL is

$$\delta\int_{S_0} ds\Phi = \int_{-\infty}^{+\infty} dx[\Phi|_{y=y_1}\delta y_1 - \Phi|_{y=y_2}\delta y_2] + \int_{S_0} ds\delta\Phi \tag{C.3}$$

where δy_1, δy_2, and $\delta\Phi$ are the first variations of respective functions. In particular

$$\delta y_k \equiv \frac{dy_k}{dx}\delta L \approx y_k(x + \delta L) - y_k(x) \tag{C.4}$$

By using eqs C.2 and C.4 one derives

$$\int_{-\infty}^{+\infty} dx[\Phi|_{y=y_1}\delta y_1 - \Phi|_{y=y_2}\delta y_2] = -\int_{x_4}^{x_3} dx\Phi|_{y=y_1(x)}\delta y_1 - \int_{x_3}^{x_4} dx\Phi|_{y=y_2}\delta y_2 = -\oint_{C_2} dl\frac{dy}{dl}\Phi\delta L \tag{C.5}$$

From eqs 4.6, C.3, and C.5 one obtains

$$\delta\Omega = \int_{S_0} ds\delta\Phi - \int_{C_2} dl\frac{dy}{dl}\Phi\delta L + \sum_{k=1}^{2}\oint_{C_k} dl(\omega_{k,\mathrm{I}} - \omega_{k,\mathrm{II}})\delta\zeta_k \tag{C.6}$$

where

$$\begin{aligned} \delta\zeta_1 &= \delta\zeta(x,y) \quad \text{for } (x,y) \in C_1 \\ \delta\zeta_2 &= \delta\zeta(x,y) \quad \text{for } (x,y) \in C_2' \end{aligned} \tag{C.7}$$

Further one derives

$$\delta\Phi = \frac{\partial\Phi}{\partial\zeta}\delta\zeta + \frac{\partial\Phi}{\partial\zeta_x}\frac{\partial}{\partial x}(\delta\zeta) + \frac{\partial\Phi}{\partial\zeta_y}\frac{\partial}{\partial y}(\delta\zeta) \tag{C.8}$$

The differentiation of eq 4.7 yields

$$\frac{\partial\Phi}{\partial\zeta_t} = \frac{\gamma\zeta_t}{(1 + |\nabla_{\mathrm{II}}\zeta|^2)^{1/2}}$$

$$t = x, y$$

Then eq C.8 can be represented in a convariant form:

$$\delta\Phi = \frac{\partial\Phi}{\partial\zeta}\delta\zeta + \frac{\gamma(\nabla_{\mathrm{II}}\zeta)\cdot\nabla_{\mathrm{II}}(\delta\zeta)}{(1 + |\nabla_{\mathrm{II}}\zeta|^2)^{1/2}} \tag{C.9}$$

Equation C.9 can be transformed to read

$$\delta\Phi = M\delta\zeta + \nabla_{\mathrm{II}}\cdot\left[\frac{\gamma(\nabla_{\mathrm{II}}\zeta)\delta\zeta}{(1 + |\nabla_{\mathrm{II}}\zeta|^2)^{1/2}}\right] \tag{C.10}$$

where

$$M = \frac{\partial\Phi}{\partial\zeta} - \nabla_{\mathrm{II}}\cdot\left[\frac{\gamma(\nabla_{\mathrm{II}}\zeta)}{(1 + |\nabla_{\mathrm{II}}\zeta|^2)^{1/2}}\right] \tag{C.11}$$

One can check that M is identically zero: (i) in the case of *thick* film (γ = const) this follows from the Laplace equation, eq 1.9, along with eqs 1.10, 4.7, and C.11; (ii) in the case of *thin* film it follows from the generalized Laplace equation, eq 4.9, along with eqs 1.10, 4.7, 4.8, and C.11. By substituting $M = 0$ in C.10 and by using the Green theorem one derives

$$\oint_{S_0} ds\delta\Phi = -\oint_{C_k} dl\mathbf{m}\cdot\left[\frac{\gamma(\nabla_{\mathrm{II}}\zeta)\delta\zeta}{(1 + |\nabla_{\mathrm{II}}\zeta|)^{1/2}}\right] \tag{C.12}$$

where $\mathbf{m}$ is outer running unit normal; see Figure 8. In general, one has[33]

$$\delta\zeta_2 = \delta\zeta|_{C_2} + \delta\mathbf{r}\cdot(\nabla_{\mathrm{II}}\zeta)|_{C_2} \tag{C.13}$$

where $\delta\zeta_2$ is defined by eq C.7 and $\delta\mathbf{r}$ is the vector of displacement of contour C_2. In our case $\delta\mathbf{r} = (\delta L, 0)$. Besides, at contour C_1 $\delta\zeta \equiv \delta\zeta_1$, as far as the position of contour C_1 is not varied. Then from eqs 2.14, C.12, and C.13 one obtains

$$\int_{S_0} ds\delta\Phi = \oint_{C_1} dl\mathbf{m}\cdot\tilde{\mathbf{n}}\gamma\delta\zeta_1 + \oint_{C_2} dl\mathbf{m}\cdot\tilde{\mathbf{n}}\gamma(\delta\zeta_2 - \zeta_x\delta L) \tag{C.14}$$

Equations C.6 and C.14 yield

$$\delta\Omega = -\oint_{C_2} dl\left(\frac{dy}{dl}\Phi + \gamma\zeta_x\mathbf{m}\cdot\tilde{\mathbf{n}}\right)\delta L + \sum_{k=1}^{2}\oint_{C_k} dl(\gamma\cos\alpha_k + \omega_{k,\mathrm{I}} - \omega_{k,\mathrm{II}})\delta\zeta_k \tag{C.15}$$

where we have taken into account that the angle subtended between the unit vectors $\mathbf{m}$ and $\tilde{\mathbf{n}}$ is the three phase contact angle α_k:

$$\mathbf{m}\cdot\tilde{\mathbf{n}} = \cos\alpha_k \qquad \text{for } (x,y) \in C_k, \quad k = 1, 2 \tag{C.16}$$

Below we will set the last term in eq C.15 equal to zero because (i) at boundary condition of *fixed contact angle* the Young equation, eq 1.14, holds, or (ii) at boundary condition of *fixed contact line* eq 1.16 holds and hence $\delta\zeta_K \equiv 0$. From eqs 4.7 and C.15 one deduces the sought for eq 4.10.

Appendix IV. Capillary Interaction Energy, $\Delta\Omega$, in the Presence of Disjoining Pressure

Our purpose here is to prove the validity of the key expressions for $\Delta\Omega$, eqs 1.19 and 1.24, for *thin* films, when

(39) Eliassen, J. D. Ph.D. Thesis, University of Minnesota, 1963; University Microfilms, Ann Arbor, MI, 1983.

the effect of disjoining pressure, Π, becomes significant. We restrict our considerations to a wetting liquid film on a substrate. (The results can be quite similarly derived for a symmetrical liquid film, Figure 2f, which can be formally related as two wetting films "adsorbed" on each other.)

As earlier, we consider a film of uneven thickness (Figure 4)

$$h = l_0 + \zeta(x,y), \qquad l_0 = \text{const} \tag{D.1}$$

For small deviations from planarity, $\zeta \ll h$, $\gamma(\zeta)$ can be expanded in series:

$$\gamma = \gamma_0 + \left(\frac{\partial\gamma}{\partial h}\right)_0 \zeta + \frac{1}{2}\left(\frac{\partial^2\gamma}{\partial h^2}\right)_0 \zeta^2 + \ldots \tag{D.2}$$

Here and hereafter the subscript "0" denotes the value of the respective quantify for $\zeta = 0$. For a plane–parallel film the thermodynamics of thin liquid films yields[35]

$$\left(\frac{\partial\gamma}{\partial h}\right)_0 = -\Pi_0; \qquad \left(\frac{\partial^2\gamma}{\partial h^2}\right)_0 = -\left(\frac{\partial\Pi}{\partial h}\right)_0 \equiv -\Pi' \tag{D.3}$$

Equations D.3 can be also derived from eq 4.8 for small meniscus slope, i.e. $|\nabla_{II}\zeta|^2 \ll 1$. The combination of eqs D.2 and D.3 leads to

$$\gamma = \gamma_0 - \Pi_0\zeta - \frac{1}{2}\Pi'\zeta^2 + \ldots \tag{D.4}$$

Equation D.4 implies that $\Delta\Omega$ can be represented as a sum of terms due to the hydrostatic pressure, wetting surface energy, and meniscus surface energy[3]

$$\Delta\Omega = \Delta\Omega_p + \Delta\Omega_w + \Delta\Omega_m \tag{D.5}$$

$\Delta\Omega_m$ is determined by the expression

$$\Delta\Omega = \gamma_0[\Delta A^p - \Delta A_\infty{}^p] \tag{D.6}$$

where

$$\gamma_0\Delta A^p \equiv \int_{S_0} ds\, [\gamma(1 + |\nabla_{II}\zeta|^2)^{1/2} - \gamma_0] \tag{D.7}$$

As usual, the subscript "∞" in eq D.6 denotes the value of the respective quantity at infinite interparticle separation, $L \to \infty$; the meaning of S_0 is the same as in eq 2.7. By expanding the square root in eq D.7 in series and substituting γ from eq D.2, one derives

$$\gamma_0\Delta A^p = \int_{S_0} ds \left[\gamma_0 \frac{1}{2}|\nabla_{II}\zeta|^2 - \Pi_0\zeta - \frac{1}{2}\Pi'\zeta^2\right] \tag{D.8}$$

where higher order terms with respect to ζ are neglected. On the other hand one has

$$\gamma_0|\nabla_{II}\zeta|^2 = \gamma_0[\nabla_{II}\cdot(\zeta\nabla_{II}\zeta) - \zeta\nabla_{II}{}^2\zeta] = \gamma_0\nabla_{II}\cdot(\zeta\nabla_{II}\zeta) - \Delta\rho g\zeta^2 + \Pi'\zeta^2 \tag{D.9}$$

At the last step we used the linearized Laplace equation[3]

$$\gamma_0\nabla_{II}{}^2\zeta = (\Delta\rho g - \Pi')\zeta \tag{D.10}$$

stemming from eqs 1.10, 1.17, and D.4 for $|\nabla_{II}\zeta|^2 \ll h$.

The substitution of eq D.9 into eq D.8 yields

$$\gamma_0 A^p = \gamma_0 I - \int_{S_0} ds \left[\Pi_0\zeta + \frac{1}{2}\Delta\rho g\zeta^2\right] \tag{D.11}$$

where

$$I \equiv \frac{1}{2}\int_{S_0} ds\, \nabla_{II}\cdot(\zeta\nabla_{II}\zeta) \tag{D.12}$$

It is worthwhile noting that the terms with Π′ cancelled in the right-hand side of eq D.11. Since both ζ and $\nabla_{II}\zeta$ vanish at infinity, the integral I can be represented as a sum of linear integrals taken along the contours C_1 and C_2:

$$I = -\frac{1}{2}\sum_{k=1}^{2} \oint_{C_k} d\mathbf{l}\mathbf{m}\cdot(\zeta\nabla_{II}\zeta) \tag{D.13}$$

where $\mathbf{m}$ is a running outer unit normal to the respective contour (Figure 8).

The hydrostatic pressure contribution in eq D.5 reads

$$\Delta\Omega_p = -[\int_{V_I} P_I\, dV + \int_{V_{II}} P_I\, dV] + [\int_{V_I} P_I\, dV + \int_{V_{II}} P_I\, dV]|_{L=\infty}$$

By means of eqs 1.3, 4.2, and 4.3 one derives

$$\Delta\Omega_p = \int_{S_0} ds \left[(P_{II,0} - P_{I,0})\zeta + \frac{1}{2}\Delta\rho g\zeta^2\right] + \text{const} \tag{D.14}$$

where the additive constant is independent of L. In addition, for an equilibrium thin liquid film one has[35]

$$\Pi_0 = P_{II,0} - P_{I,0} \tag{D.15}$$

Then a combination of eqs D.5, D.6, D.11, D.14, and D.15 yields

$$\Delta\Omega = \gamma_0(I - I_\infty) + \Delta\Omega_w \tag{D.16}$$

Note that the integrals throughout S_0 in eqs D.11 and D.14 cancel each other.

In the case of *constant contact angle* eq 1.15 holds. Then for two identical particles one obtains[3] ($\cot\alpha_k = \tan\Psi_c \approx \sin\Psi_{c\infty}$)

$$I = 2\pi r_c h_c \sin\Psi_{c\infty}, \qquad h_c \equiv \frac{1}{2\pi r_c}\oint_{C_1} dl\zeta \tag{D.17}$$

In addition, for the same case one can derive[3]

$$\Delta\Omega_w = -4\pi\gamma_0 r_c(h_c - h_{c\infty})\sin\Psi_{c\infty} \tag{D.18}$$

Finally, a combination of eqs D.16–D.18 leads to eq 1.19 with γ_0 instead of γ. The difference between γ and γ_0 is of the order of Πh and is negligible compared to γ; see e.g. ref 35.

In the alternative case of *fixed contact line* one has $\Delta\Omega_w = 0$. Moreover, eq 1.16 implies that

$$I = 2\pi r_c h_{c\infty}\sin\Psi_c, \qquad \sin\Psi_c \equiv \frac{-1}{2\pi r_c}\oint_{C_1} d\mathbf{l}\mathbf{m}\cdot\nabla_{II}\zeta \tag{D.19}$$

Then eq D.16 reduces to eq 1.24.

Similarly one can confirm the validity of eq 5.4 for partially immersed spheres (instead of cylinders).

The absence of an explicit term with the disjoining pressure Π in eqs 1.19 and 1.24 does not mean that $\Delta\Omega$ is independent of Π. In fact Π affects $\Delta\Omega$ implicitly, through the values of h_c or Ψ_c, which are determined by solving the Laplace equation, eq D.10. Indeed, the latter contains a Π′ term.